論文 / 著書情報
Article / Book Information

Title	APPLICATION OF NEW BENDING-SHEAR MODEL FOR SIMPLIFIED ANALYSIS OF VARIOUS SUPER-TALL BUILDINGS
Authors	K. Watai, K. Kasai, S. Maeda, D. Sato, Y. Suzuki
Pub. date	2020, 9
Citation	2020 17WCEE Proceedings

17th World Conference on Earthquake Engineering, 17WCEE
Sendai, Japan - September 13th to 18th 2020

APPLICATION OF NEW BENDING-SHEAR MODEL FOR SIMPLIFIED ANALYSIS OF VARIOUS SUPER-TALL BUILDINGS

K. Watai[(1)], K. Kasai[(2)], S. Maeda[(3)], D. Sato[(4)], Y. Suzuki[(5)]

[(1)] *Specially Appointed Assistant Professor, Tokyo Institute of Technology, watai.k.aa@m.titech.ac.jp*
[(2)] *Specially Appointed Professor, Tokyo Institute of Technology, kasai.k.ac@m.titecha.c.jp*
[(3)] *Takenaka Corporation, maeda.shuusaku@takenaka.co.jp*
[(4)] *Associate Professor, Tokyo Institute of Technology, sato.d.aa@m.titech.ac.jp*
[(5)] *Takenaka Corporation, suzuki.yousuke@takenaka.co.jp*

Abstract

When a super-tall building is designed, a member-to-member model is constructed to represent the assembly of columns, beams, walls and so on. The seismic response analysis using this model is computationally expensive and outputs large amount of data. Therefore, an equivalent mass-spring system with a small number of elements and short analysis time is useful at the initial design stage. Since the influence of bending deformation becomes large as building becomes taller, it must be simulated by the equivalent mass-spring system. The companion paper (Kasai et al. 2020) therefore proposed a simplified method to formulate such an equivalent system, and named it as the bending-shear model. In this paper, we extend the modeling method to and verify the model accuracy for various super-tall buildings.

We consider four different buildings heights from 80m to 400m, as well as three different structural systems such as moment resisting system, center core system, and outrigger system combined with center core. The method can be easily applied to these various frame types because the bending stiffness is calculated using only horizontal displacement given as the overall responses, in contrast to existing method that considers deformations of all the vertical members. Note however that the analysis using pure moment discussed in the companion paper is modified to cover different systems mentioned above, considering their distinct distributions of column axial deformations.

For the different systems, the bending stiffness of the bending-shear model under the distributed story moments and shear forces consistently appears to be smaller than that under the pure moment. As such, its second and third frequencies and mode vectors match with those of the member-to-member model regardless of the structural system considered. For the variety of the buildings, we confirmed that the displacement, story drift and acceleration time-history responses of the bending-shear model agree remarkably well with those of the member-to-member models.

Keywords: Super tall building; Mass-spring system; Bending-shear model; Vibration period; Mode vector

1. Introduction

For super tall buildings of increasing height, it has been demanded to develop the seismic analysis using simplified model. In the design procedure, detailed dynamic characteristics of the building will be verified using member-to-member model that constructed each member (columns, beam, and brace et al.) individually. However, the analytical studies for various parameters on initial design term takes too long using this model. Therefore, it is desirable to analyze using a simplified model in initial term, and using member-to-member (M) model as a final confirmation analysis.

A simplified model is divided into two types; the first is shear model where the bar deforms in shear. The second is bending-shear model where the bar deforms in both shear and bending. The shear (S) model has fine modeling accuracy for low- / middle-rise buildings and the bending shear (B) model has fine modeling accuracy for low- to high-rise buildings. The super tall buildings have been replaced with simplified system in some studies [1 to 3]. However, the model has been constructed with the specifications in the design documents, and most of target buildings are moment frame structure. There are few studies of the modeling accuracy and the application limit used simplified model. Therefore, there are still problems with using simplified model to super tall buildings for increasing height. There is a method of *Muto* et al. [4, 5] that is often used to evaluating the bending stiffness of B model, but its application is limited to moment frame structure. The simplified model applicable to complex structural model has still not been proposed.

The companion paper by *Kasai et al.* [6] proposed a simplified modeling method to formulate such an equivalent system, and named it as the bending-shear ($B^{(1)}$) model. In this paper, we extend the modeling method and verify the model accuracy for various super tall buildings.

2. Modeling method for bending shear model and example buildings

2.1 Modeling procedure

In this paper, the model name is below following the companion paper, called the Member- to-member model as M model, and called the propose bending shear model as $B^{(1)}$ model. Before the below modeling procedure, it obtains the circular frequency ω_1 and the each layer horizontal eigenvector ϕ_1 of first obtained from eigenvalue analysis of M model. Then, it calculates the story eigenvector $\Delta\phi_{i1} = \phi_{i1} - \phi_{i-1,1}$. In addition, The first mode overturning moment $Mi^{(1)}$ and the shear force $Q_i^{(1)}$ is obtained from following equations;

$$Q_i^{(1)} = \sum_{k=i}^{n} F_k^{(1)} = \omega_1^2 \sum_{k=i}^{n} (m_k \phi_{k1}) \quad , \quad M_i^{(1)} = \sum_{k=i}^{n} (Q_k^{(1)} h_k) \tag{1a, b}$$

The drift $\Delta\phi_{i1}$ of the first mode eigenvector is decomposed into bending and shear drifts $\Delta\phi_{bi1}$ and $\Delta\phi_{si1}$, respectively.

$$\Delta\phi_{i1} = \Delta\phi_{bi1} + \Delta\phi_{si1} \tag{2}$$

The procedure uses M-model analysis in steps 1 to 3, and $B^{(1)}$-model analysis in steps 4 and 5 as follows:

1) Obtain horizontal displacement u_{bi} due to the bending moment M_0 applied at the top of M-model (Pure moment loading analysis). Vertical forces of equal magnitude are applied to all the columns sharing the plane perpendicular to the horizontal force direction, where the plane developing the largest sum of the column axial forces at the 1st story under typical horizontal loading.
2) Obtain the curvature p_i by using u_{bi} and following equation (2) where.

$$p_i = \left\{\Delta u_{bi} - (h_i / h_{i-1})\Delta u_{b,i-1}\right\} \Big/ h_i^2 \tag{3}$$

where $\Delta u_{bi} = u_{bi} - u_{b,i-1}$, $h_i = H_i - H_{i-1}$ = floor height, and $u_{b0} = H_0 = \theta_1 = 0$ when calculating for the 1st story.

3) Obtain bending stiffness EI_i from p_i and adjustment factor α. For the first iteration, $\alpha = 1$ may be assumed.

$$EI_i = \alpha M_0 / p_i \tag{4}$$

4) The increment rotation angle $\Delta\theta_i$ and the bending drift $\Delta\phi_{bi}$ of first mode are obtained from the first mode overturning moment $M_i^{(1)}$, $M_{i+1}^{(1)}$.

$$\Delta\theta_{i1} = \frac{h_i}{2EI_i}(M_i^{(1)} + M_{i+1}^{(1)}), \quad \Delta\phi_{bi1} = \frac{h_i^2}{6EI_i}(2M_i^{(1)} + M_{i+1}^{(1)}) + h_i \sum_{k=1}^{i-1} \Delta\theta_{k1} \tag{5a, b}$$

Obtain the shear stiffness K_{si} using equations (4) and (5).

$$K_{si} = Q_i^{(1)} / \Delta\phi_{si1} \tag{6}$$

5) After creating $B^{(1)}$ model based on steps 3) and 4), conduct its eigenvalue analysis. Confirming the 1st mode properties match with those of M model, and iterate for the 2nd mode properties by repeating steps 3 to 5. Typically, α is reduced until convergence, and it appears to be around 0.8 for the buildings considered in this study. If a negative shear stiffness K_{si} is obtained in this procedure, use the minimum α-value that hold $K_{si} > 0$.

2.2 Overview of example buildings

Figure 1 shows the four building models used in this study. These models are assumed to be the super tall building with a height of 80 to 400m and an aspect ratio of 1.6 to 8.0. The 80m model is a 20-story theme structure (trim type) designed in Ref. [7], and the 150m model is referenced an existing building model [8]. These building models are constructed with moment frame (Hereinafter, called this model "Moment frame model"). The 300m and 400m models are designed for this study, assuming the highest or higher super tall buildings in Japan at present. Both models are constructed with a center core structure and outrigger structure referenced overseas super tall buildings (Hereinafter, called this model "Core + Outrigger frame model") [9]. In this study, the applicability of proposed method is verified to various frame type by attaching or removing brace to above building models. First, it construct a center core structure of 80m model (Hereinafter, called this model "Core frame model"). This model is attached braces in X4~6 frame of Y2 and Y3 (figure 2). The

Model		80m	150m	300m	400m
Height	(m)	82.0	146.1	300.0	400.0
Plan	(m)	51.2 × 35.2	64.8 × 28.8	50.0 × 50.0	50.0 × 50.0
Aspect ratio	-	1.6	2.3	6.0	8.0
Story	-	20	37	60	80
1st mode natural period	(s)	3.648	4.852	5.288	6.938
Natural period / Height	(s/m)	0.044	0.033	0.018	0.017

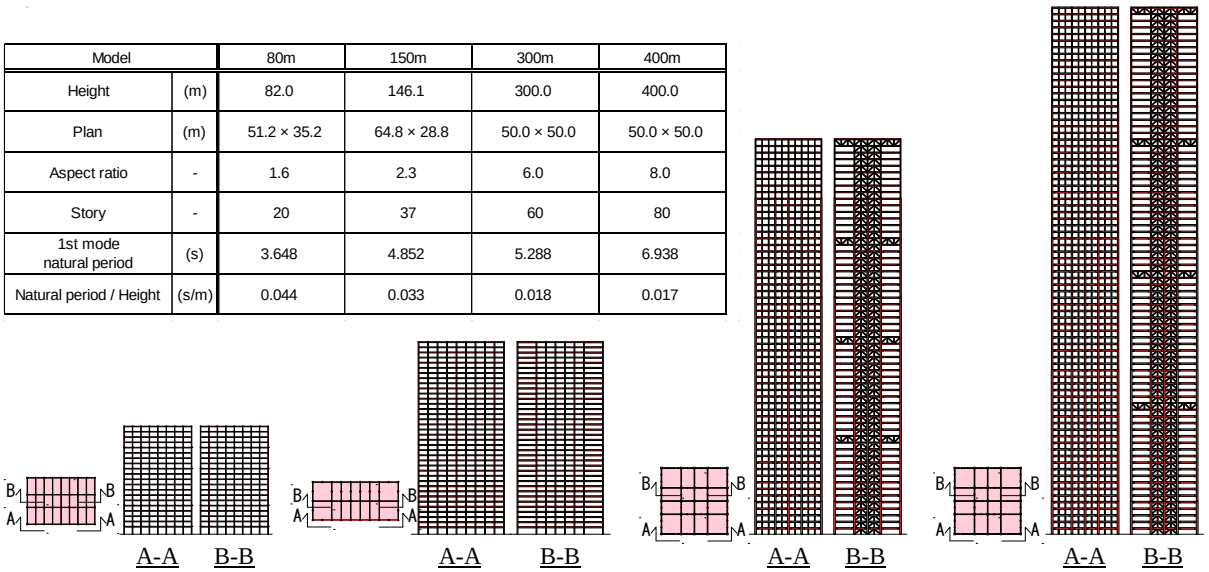

a) 80m mode (20-story) b) 150m mode (37-story) c) 300m mode (60-story) d) 400m mode (80-story)

Fig. 1 – Building plans and elevations

section area of these braces is 0.5 times the ceiling beam in each layer. Similarly, Core frame model of 300m and 400m model construct with removing outrigger structure and seismic studs. In addition, Moment frame model of 300m and 400m model construct with removing core structure from Core frame model. It considered using all 9 models above. The above 9 models are used in this study. Both models consider the translational component of X direction and the members are elastic.

2.3 Pure moment loading method

This section shows the pure moment loading method for various frame types. Figure 2 shows plans and the distribution of the columns axial forces at first layer under loading the horizontal force. These forces are the sum of the columns arranged on each X-plane shown figure 2. The moment frame and Core + Outrigger frame model occurred maximum and minimum axial forces at the outermost edge regardless of building height. In the case of Core frame of 80m model, the axial forces are maximum and minimum at the end of core structure (X4, 6). In the other hand, 300m and 400m Core model occurred these values at the outermost edge. As the same time, the axial forces at the end of core frame has a tendency of being large even in 300m and 400m model. However, the axial forces at the outermost edge is larger than edge of core for the building is higher and higher. As shown in the modeling procedure step 1, the vertical forces for loading pure moment is applied to all the columns arranged in the frame where the axial forces were maximum and minimum. In this way, the proposed method can be applied to various frame type by selecting the loading points. For example, figure 3 shows a conceptual diagram of the pure moment loading method and deformation mode for 80m models. Because of this, the vertical forces to loading pure moment were applied at the outermost edge for all models except 80m Core frame model in this study.

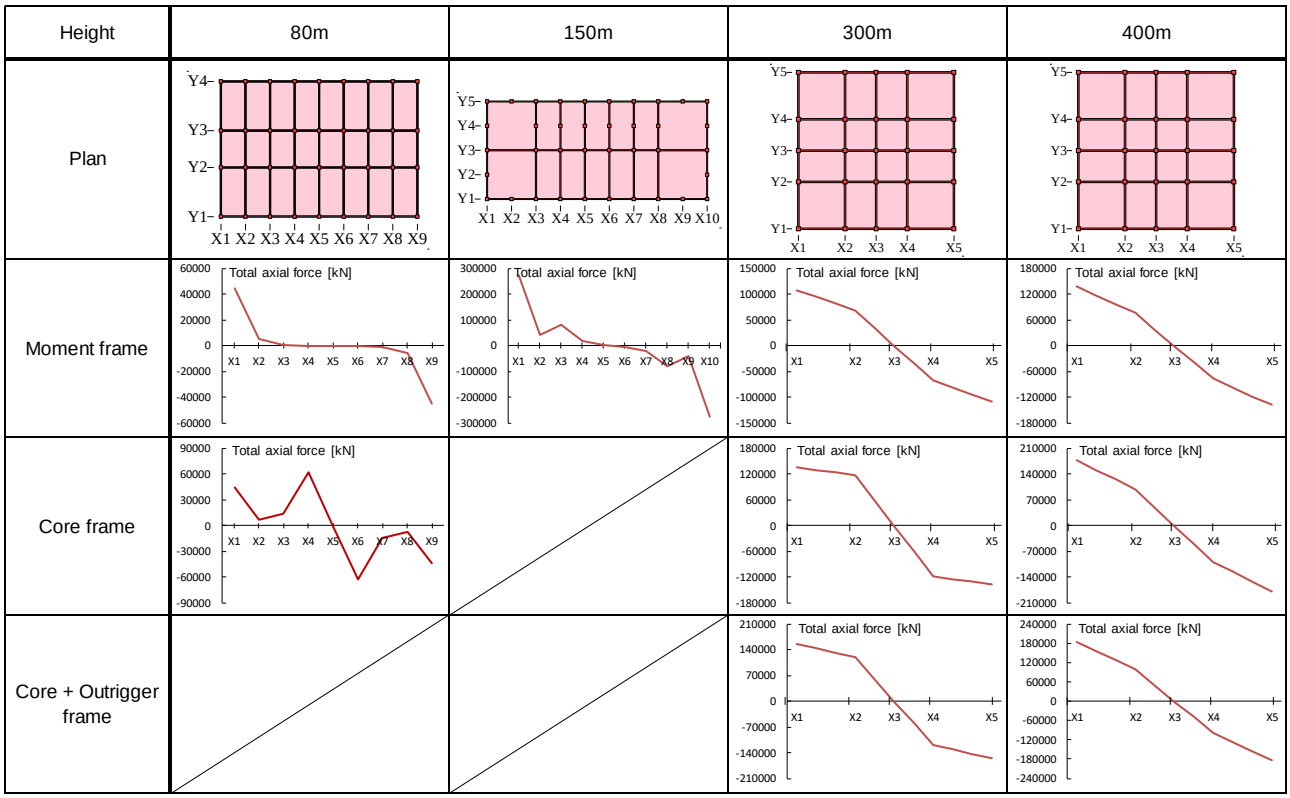

Fig. 2 – Distribution of axial force under horizontal forces

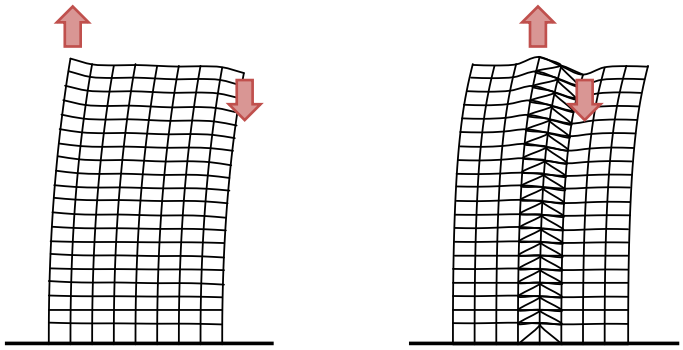

a) Moment frame model b) Core frame model

Fig. 3 – Conceptual diagram of pure moment loading methods of 80m model

2.4 Correction of curvature and shear stiffness

In this section, it shows a correcting way for the case that obtained negative curvature or shear stiffness. When loading a moment to the tip of the cantilever, the bending displacement generally increases from the fixed end toward the tip. However, in the case of the buildings constructed with the outrigger frame, the story drift may not increase in these layers even if displacement increases. For the reasons, the curvature obtained from equation (3) was negative value ($p_{46} < 0$) in 46th-layer of 300m Core + Outrigger frame model. Reverse bending effect causes reverse shear forces to the column in M model, but this behavior cannot be expressed by bending shear model. Therefore, this method assuming that the curvature of building model increases gradual as well as cantilever under loading pure moment. The negative curvature of i-th layer is corrected by giving the curvature of lower layer $p_i = p_{i-1}$. In addition, negative curvature was also calculated in an 80th layer of 400m Core frame in this study, because the frame with many braces show unstable behavior near the top layer where the vertical forces loading. The correction for this is the same as before.

The modeling procedure step 5 shows that the adjusting factor α calibrate to hold $K_{si} > 0$. However, a negative shear stiffness will be allowed when the building has the reverse bending effect as outrigger frame. Specifically, the layer which the negative shear stiffness have been obtained from equation (6) is given shear stiffness as large as possible. In this study, the negative shear stiffness was obtained from 60th layer of 300m Core + Outrigger frame model and 80th layer of 400m Core + Outrigger frame model when calibrating bending stiffness. Nevertheless, no negative stiffness was calculated for the other layer when the correction coefficient was reduced until the second natural period match to M model. Additionally, the high modeling accuracy is obtained even if correcting curvature and shear stiffness as shown later section.

3. Model accuracies for dynamic properties

This verifies accuracy of $B^{(1)}$ model for simulating vibration periods and participation for 9 building models shown in section 2.2. Table 1 shows the natural periods, the relative error of natural period to M model and the adjusting factor α. In addition, figure 4 shows participation vector $\beta_j \phi_{ij}$ which the product of the participation coefficient β_j defined by equation (7) and the eigenvector ϕ_{ij}, and its drift $\beta_j \Delta \phi_{ij}$.

$$\beta_j = \boldsymbol{\phi}_j^T \mathbf{M1} \Big/ \boldsymbol{\phi}_j^T \mathbf{M} \boldsymbol{\phi}_j \tag{7}$$

Where, j = mode order, $\mathbf{M}$ = mass matrix and subscript T indicates transportation.

For the model in this study, the adjusting value were in the range of 0.605 to 0.840, and these tended to decrease as the aspect ratio increased. As shown table 1, the first and second natural periods of $B^{(1)}$ model were matched M model. In the case of simple Moment frame model, the high modeling accuracy was obtained for

Table 1 – Comparison of natural periods

Height		80m				150m	
Construction		Moment frame		Core frame		Moment frame	
α		-	0.790	-	0.605	-	0.840
mode	1	3.648	3.648 (+0.0%)	2.791	2.791 (+0.0%)	4.852	4.852 (+0.0%)
	2	1.357	1.357 (+0.0%)	0.980	0.980 (+0.0%)	1.684	1.684 (+0.0%)
	3	0.811	0.817 (+0.8%)	0.551	0.540 (-2.0%)	0.999	1.007 (+0.7%)
	4	0.576	0.589 (+2.2%)	0.383	0.377 (-1.6%)	0.710	0.725 (+2.1%)
	5	0.436	0.455 (+4.3%)	0.291	0.288 (-1.1%)	0.534	0.557 (+4.3%)

Height		300m					
Construction		Moment frame		Core frame		Core + Outrigger frame	
α		-	0.770	-	0.687	-	0.754
mode	1	7.491	7.491 (+0.0%)	5.542	5.542 (+0.0%)	5.288	5.288 (+0.0%)
	2	2.504	2.504 (+0.0%)	1.695	1.695 (+0.0%)	1.611	1.611 (+0.0%)
	3	1.402	1.414 (+0.9%)	0.877	0.925 (+5.5%)	0.838	0.871 (+3.9%)
	4	0.969	0.985 (+1.7%)	0.575	0.644 (+12.0%)	0.565	0.612 (+8.3%)
	5	0.733	0.751 (+2.4%)	0.422	0.497 (+17.7%)	0.391	0.440 (+12.5%)

Height		400m					
Construction		Moment frame		Core frame		Core + Outrigger frame	
α		-	0.766	-	0.761	-	0.759
mode	1	8.987	8.987 (+0.0%)	7.040	7.040 (+0.0%)	6.938	6.938 (+0.0%)
	2	2.961	2.961 (+0.0%)	2.201	2.201 (+0.0%)	2.152	2.152 (+0.0%)
	3	1.605	1.612 (+0.4%)	1.156	1.181 (+2.2%)	1.133	1.143 (+0.9%)
	4	1.099	1.110 (+1.0%)	0.771	0.810 (+5.0%)	0.765	0.785 (+2.5%)
	5	0.831	0.842 (+1.3%)	0.568	0.618 (+8.8%)	0.544	0.570 (+4.7%)

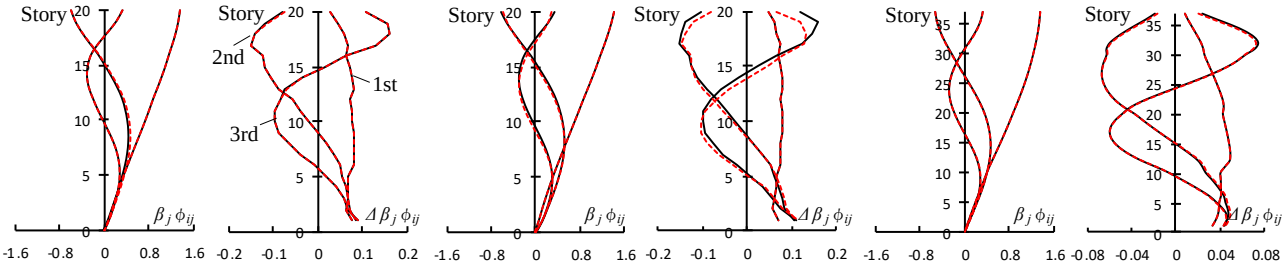

a) 80m Moment frame b) 80m Core frame c) 150m Moment frame

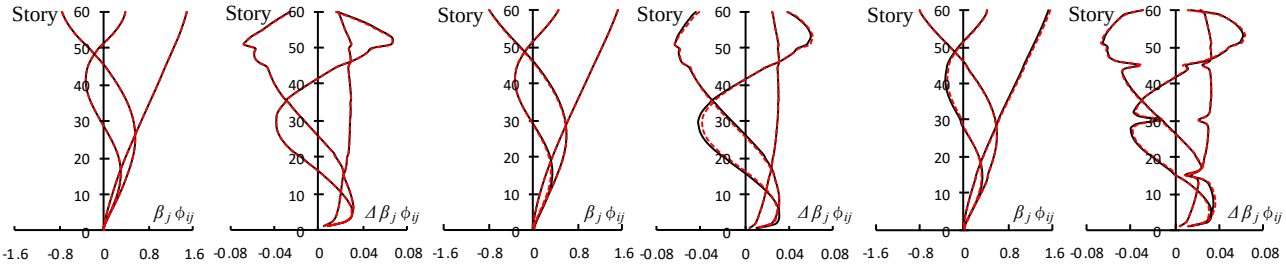

d) 300m Moment frame e) 300m Core frame f) 300m Core + Outrigger frame

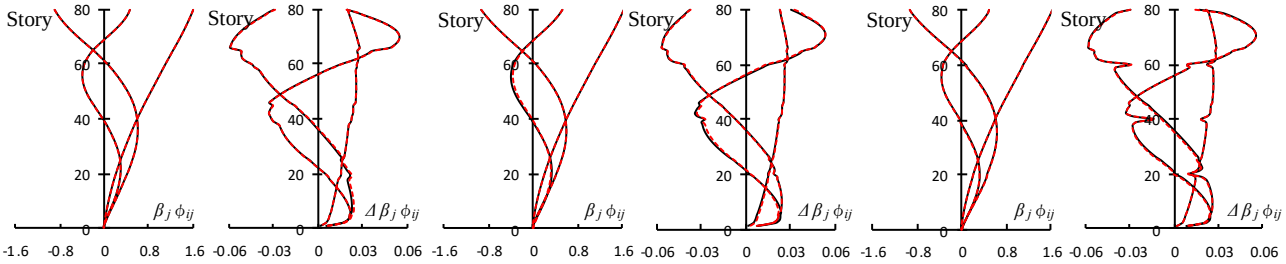

g) 400m Moment frame h) 400m Core frame i) 400m Core + Outrigger frame

—— M model ---------- $B^{(1)}$model

Fig. 4 – Comarison of participation vectors (Left:Displacement Right:Story drift)

the relative error of the fifth mode is within 5%. On the other hand, in the case of more complicated frame model, the relative error in the fifth mode exceeds 10%. At the same time, the participation vector of all models matched M model fairly well when evaluating by the displace components. When evaluating by drift, the tendency that $\beta_j \Delta \phi_{ij}$ became smaller in outrigger layer can be reproduced for Core + Outrigger frame model. However, in the case of Core frame model, the modeling accuracy was lower than the other models. In the next section, it confirms that the effect of these modeling accuracy on seismic response.

4. Model accuracies for earthquake responses

4.1 Comparison between M model and $B^{(1)}$ model

Figure 5 shows the maximum response values which are acceleration, displacement, story drift angle and shear force of 400m Core frame model and figure 6 shows 400m Core + Outrigger frame model when the BCJ-L2 wave and The Southern Hyogo Prefecture Earthquake in 1995 recorded KOBE in north-south component wave (Hereinafter, JMA-KOBE). In addition, figure 7 shows time histories of 400m Core + Outrigger frame model. Note, the structural damping is $h_1 = h_2 = 0.02$ of Rayleigh damping for 400m models.

The analysis results of $B^{(1)}$ model matched M model fairly well. The modeling accuracy of the acceleration responses was fine because the modeling accuracy for the higher-order mode was fine. As for the time histories, the overall phase and the vibration of sort-term can be reproduced response of M model. Therefore, not only the maximum response values but also the time occurred were matched. Because of this, it was confirmed that the high modeling accuracy also gets using proposed method for complicated buildings.

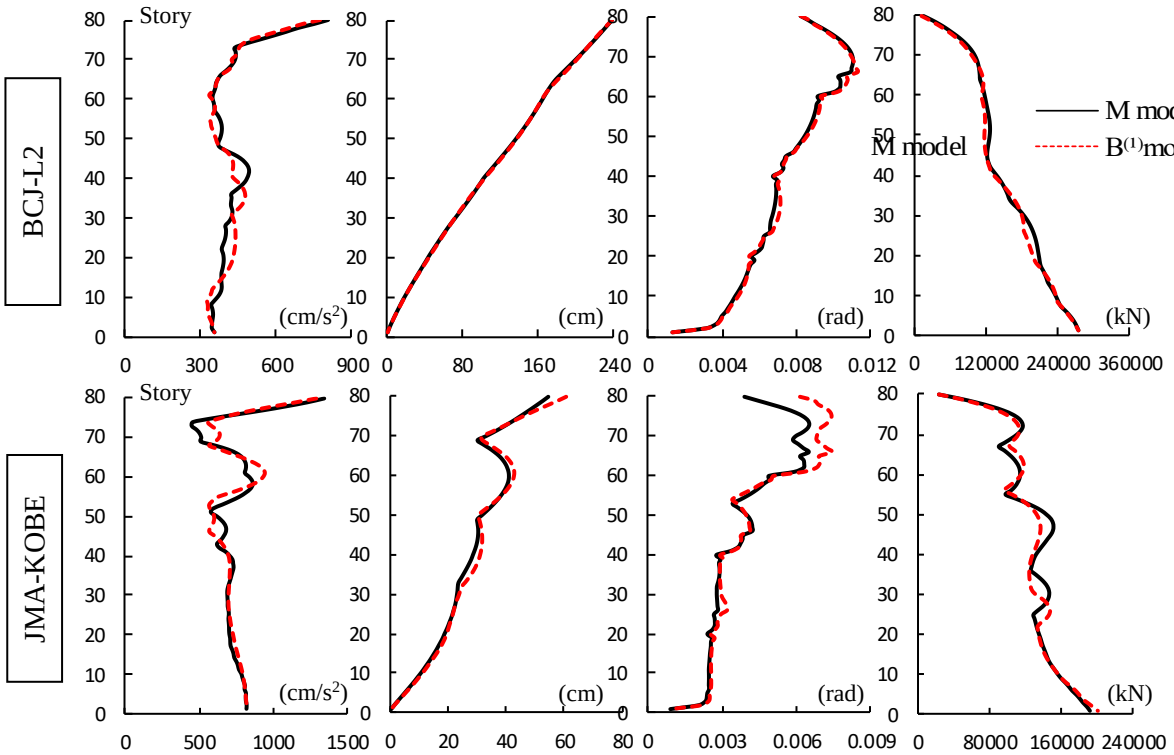

a) Acceleration b) Displacement c) Story drift angle d) Shear force

Fig. 5 – Comarison of maximum responses (400m Core frame model)

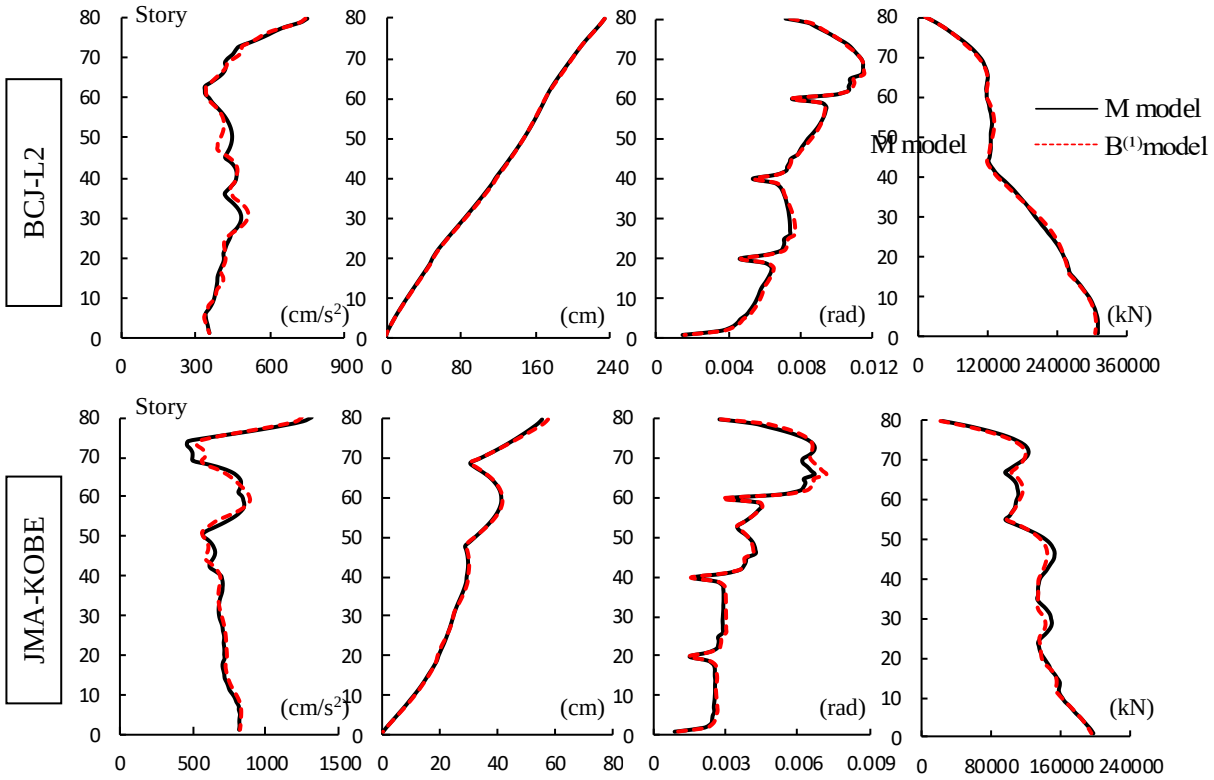

a) Acceleration b) Displacement c) Story drift angle d) Shear force

Fig.6 – Maximum responses (400m Core + Outrigger frame model)

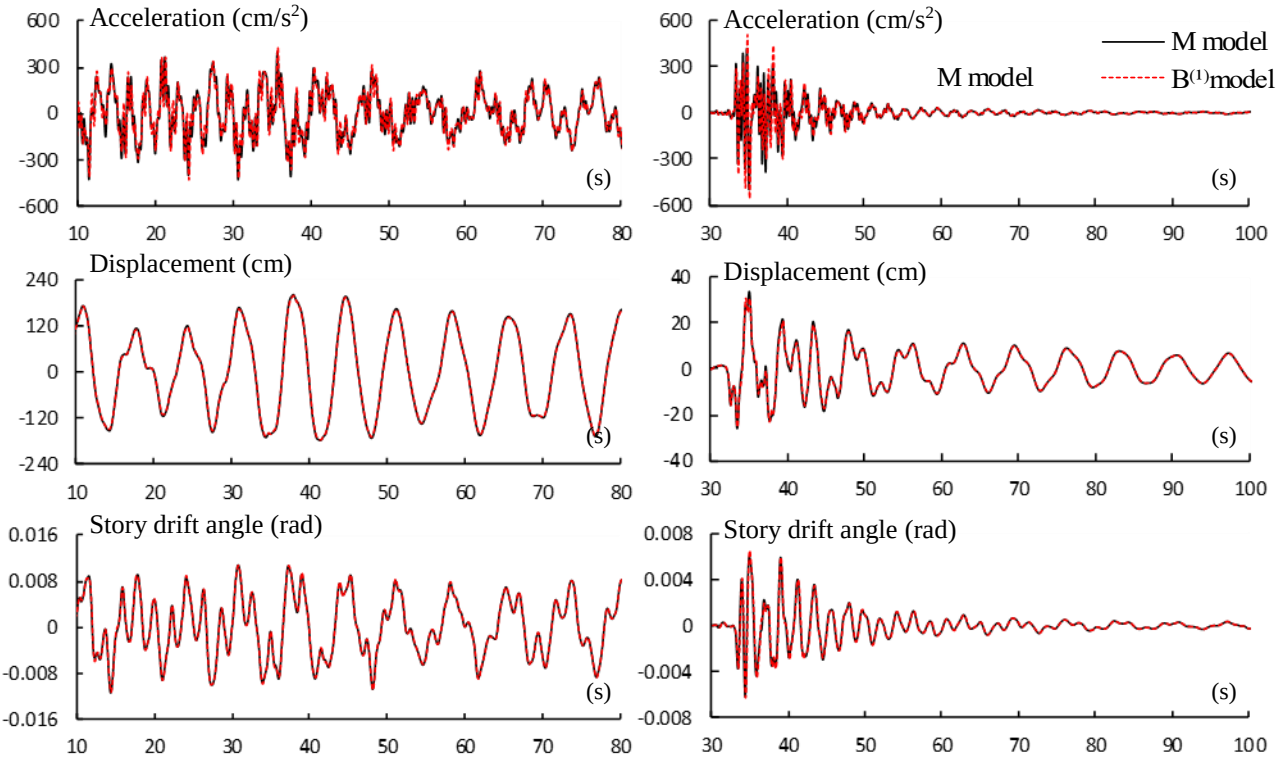

a) BCJ-L2 b) JMA-KOBE

Fig.7 – Time response histories (70th story of 400m Core + Outrigger frame model)

4.2 Comparison between frame types of B(1) model

In this section, it compares the seismic responses due to differences in frame type of the 400m model. It separates the story drift of B(1) model into bending and shear components. Figure 8 shows the time histories of the story drift in 70th layer when the BCJ-L2 wave and JMA-KOBE wave are input. As Figure 8a shows, the bending component shown in red line is larger than the shear component shown blue line for all models for BCJ-L2. This extent is larger in Core frame model and Core + Outrigger frame model than Moment frame model. In addition, the shear component had a short-term vibration which is influenced by high-order modes, but its influence is small for the bending component. On the other hand, for the JMA-KOBE wave shown in Figure 8b, the shear component is larger than the bending component even in the 70th layer.

Figure 9 shows the seismic response spectrum. JMA-KOBE wave has larger response value than BCJ-L2 wave in short-period. Therefore, the first mode in BCJ-L2 wave and the second and third modes in JMA-KOBE wave mainly affects the overall response. Figure 10 shows bending and shear components of eigenvector obtained from equation (1), (2) and (5). The bending component in first mode and the shear component in second and third modes was relatively large. Therefore, it is considered that the bending component became large due to the first mode for BCJ-L2 wave, and the shear component became large due to the second and third modes for JMA-KOBE wave. Furthermore, the ratio of bending component in story drift $\Delta u_{b,i}$ of Core and Core + Outrigger frame model was larger than Moment frame model since its component $\Delta \phi_{bi}$ of Core and Core + Outrigger frame model is larger than Moment frame model. In higher-order mode, there was no remarkable difference of shear and bending components depending on the frame types.

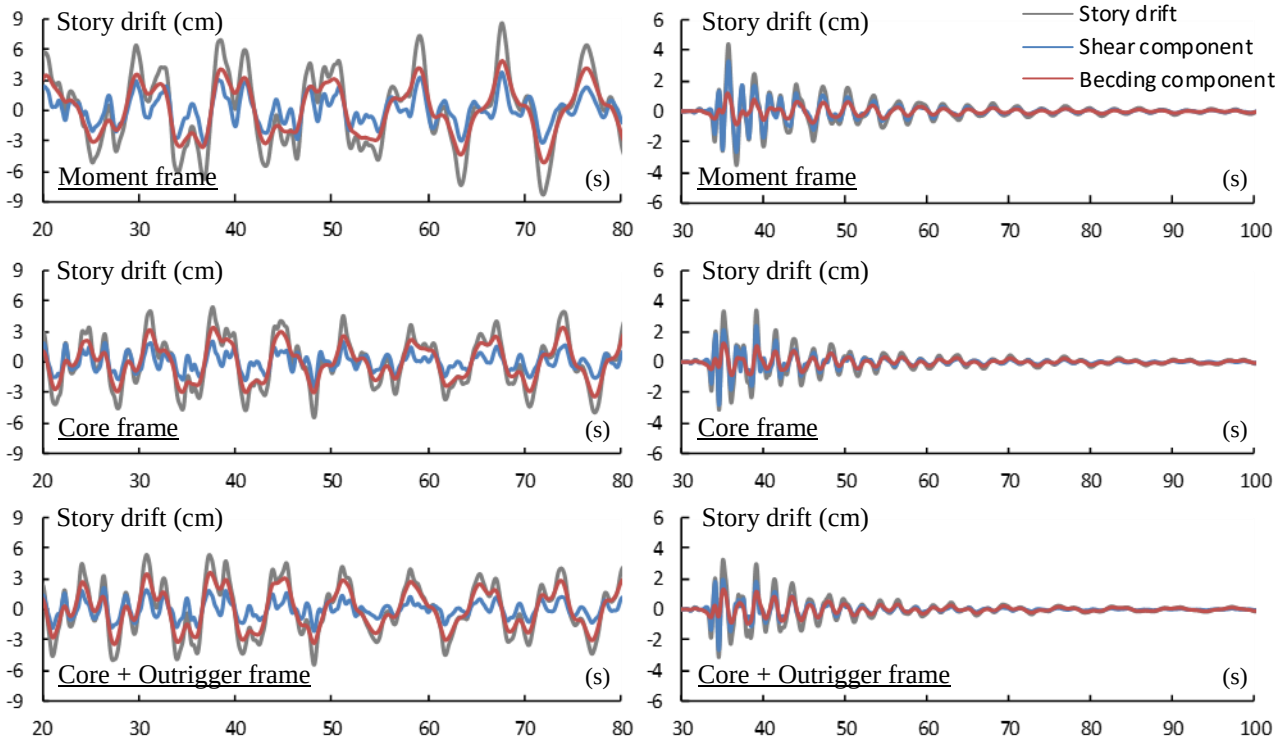

a) BCJ-L2 b) JMA-KOBE

Fig. 8 – Separation into shear and bending component of story drift (70th story of 400m B(1) model)

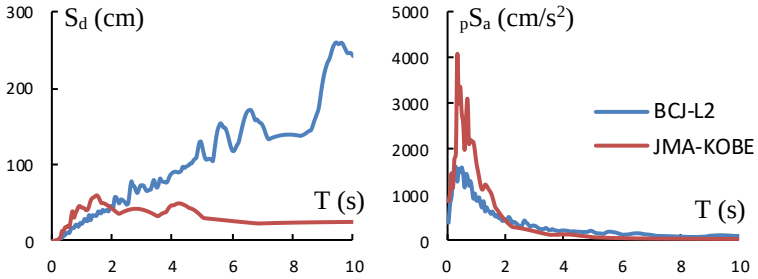

a) Displacement b) Pseudo Acceleration

Fig.9 – Response spectrum (h=0.02)

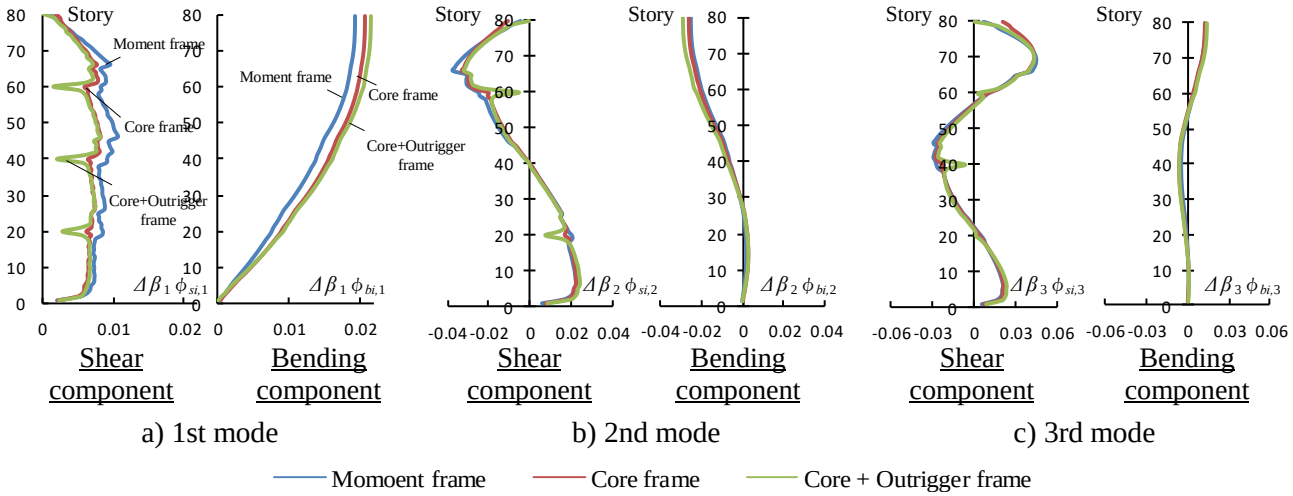

a) 1st mode b) 2nd mode c) 3rd mode

Momoent frame Core frame Core + Outrigger frame

Fig. 10 – Separation into shear and bending component of participation vector (400m B(1) model)

5. Conclusion

In conclusion, the modeling accuracy of a new bending shear modeling method is verified to apply to various height and frame type building models. These were summarized below.

(1) The proposed modeling method can be applied in consideration of the characteristics of the various building models by defining the vertical loading points for pure moment loading analysis based on the axial forces of first layer obtained from horizontal loading analysis.

(2) The bending stiffness can be easily calculated using only horizontal bending displacement obtained from pure moment loading analysis regardless of the complication of the building construction.

(3) The correction coefficient of bending stiffness tends to be smaller for the aspect ratio of building models is larger.

(4) The high modeling accuracy of seismic responses can be obtained by accurately reproduced the natural periods of the first and second modes.

Further studies are needed in order to apply to seismic response control structures and elastic-plastic frames.

6. Acknowledgements

This work was a joint research between Tokyo Institute of Technology and Takenaka Corporation, and was supported by JST Program on Open Innovation Platform with Enterprises.

7. References

[1] Okazawa R, Sugino M, Hayashi Y (2019): Modeling of super high-rise buildings and response properties against Ricker wavelet, J. Struct. Constr. Eng., AIJ, Vol.83, No.745, 421-430

[2] Morita Koichi, Hasegawa T (2016): Estimation of response and beam ends damage of steel frame high-rise buildings under long period motions, AIJ J. Technol. Des., Vol.22, No.52, 897-900

[3] Akita T, Hamada S, Sato A, Tanuma T, Yasui M, Yamamoto T, Izumi N (2013): A Study on Vibration Model using Seismic Response Evaluation of High-rise RC Building : Part 1. Comparison of Evaluation Result and Seismic Record, Summaries of Technical Papers of Annual Meeting, Architectural Institute of Japan, Structures-IV, 1-4

[4] Osawa Y, Minami T, Matsushima Y, Nagata M (1981): Kenchikugakutaikei38 Kozo no Douteki Kaiseki, SHOKOKUSHA Publishing Co., 222-224

[5] Muto K, Nagata M, Ueno H, Kanayama H, Hanajima M (1979): Earthquake response analysis system of highrise buikding: “FAPP-FASP” system, The 1st Electronic Computer Symposium, 205-210

[6] Kasai K, Watai K, Maeda S, Sato D, Suzuki Y (2020); Development of Bending-shear model for Simplified Analysis of Super-tall Buildings, 16WCEE, Sendai, JAPAN.

[7] The Japan Society of Seismic isolation (2013); Manual for Design and Construction of Passively-Controlled Buildings (3rd Edition), 131-152

[8] Ueno F, Watai K, Sato D, Kasai K, Saburi K, Maeda T, Masuda H (2020): Seismic retrofit design using a combination of oil dampers and displacement controllers for an existing tall building against extreme ground motion, Journal of Structural Engineering, Vol.66B

[9] M.Nicoreac, J.C.D.Hoenderkamp (2012): Periods of vibration of braced frames with outriggers, Steel Structures and Bridges 2012, Procedia Engineering, Vol.40, 298-303

